

Search for neutral Higgs bosons in multi- b -jet events in $p\bar{p}$ collisions at $\sqrt{s} = 1.96$ TeV

V.M. Abazov³⁶, B. Abbott⁷⁵, M. Abolins⁶⁵, B.S. Acharya²⁹, M. Adams⁵¹, T. Adams⁴⁹, E. Aguilo⁶, S.H. Ahn³¹, M. Ahsan⁵⁹, G.D. Alexeev³⁶, G. Alkhazov⁴⁰, A. Alton^{64,a}, G. Alverson⁶³, G.A. Alves², M. Anastasoie³⁵, L.S. Ancu³⁵, T. Andeen⁵³, S. Anderson⁴⁵, B. Andrieu¹⁷, M.S. Anzelc⁵³, M. Aoki⁵⁰, Y. Arnoud¹⁴, M. Arov⁶⁰, M. Arthaud¹⁸, A. Askew⁴⁹, B. Åsman⁴¹, A.C.S. Assis Jesus³, O. Atramentov⁴⁹, C. Avila⁸, F. Badaud¹³, A. Baden⁶¹, L. Bagby⁵⁰, B. Baldin⁵⁰, D.V. Bandurin⁵⁹, P. Banerjee²⁹, S. Banerjee²⁹, E. Barberis⁶³, A.-F. Barfuss¹⁵, P. Bargassa⁸⁰, P. Baringer⁵⁸, J. Barreto², J.F. Bartlett⁵⁰, U. Bassler¹⁸, D. Bauer⁴³, S. Beale⁶, A. Bean⁵⁸, M. Begalli³, M. Begel⁷³, C. Belanger-Champagne⁴¹, L. Bellantoni⁵⁰, A. Bellavance⁵⁰, J.A. Benitez⁶⁵, S.B. Beri²⁷, G. Bernardi¹⁷, R. Bernhard²³, I. Bertram⁴², M. Besançon¹⁸, R. Beuselinck⁴³, V.A. Bezzubov³⁹, P.C. Bhat⁵⁰, V. Bhatnagar²⁷, C. Biscarat²⁰, G. Blazey⁵², F. Blekman⁴³, S. Blessing⁴⁹, D. Bloch¹⁹, K. Bloom⁶⁷, A. Boehnlein⁵⁰, D. Boline⁶², T.A. Bolton⁵⁹, E.E. Boos³⁸, G. Borissov⁴², T. Bose⁷⁷, A. Brandt⁷⁸, R. Brock⁶⁵, G. Brooijmans⁷⁰, A. Bross⁵⁰, D. Brown⁸¹, N.J. Buchanan⁴⁹, D. Buchholz⁵³, M. Buehler⁸¹, V. Buescher²², V. Bunichev³⁸, S. Burdin^{42,b}, S. Burke⁴⁵, T.H. Burnett⁸², C.P. Buszello⁴³, J.M. Butler⁶², P. Calfayan²⁵, S. Calvet¹⁶, J. Cammin⁷¹, W. Carvalho³, B.C.K. Casey⁵⁰, H. Castilla-Valdez³³, S. Chakrabarti¹⁸, D. Chakraborty⁵², K. Chan⁶, K.M. Chan⁵⁵, A. Chandra⁴⁸, F. Charles^{19,†}, E. Cheu⁴⁵, F. Chevallier¹⁴, D.K. Cho⁶², S. Choi³², B. Choudhary²⁸, L. Christofek⁷⁷, T. Christoudias⁴³, S. Cihangir⁵⁰, D. Claes⁶⁷, J. Clutter⁵⁸, M. Cooke⁸⁰, W.E. Cooper⁵⁰, M. Corcoran⁸⁰, F. Couderc¹⁸, M.-C. Cousinou¹⁵, S. Crépe-Renaudin¹⁴, D. Cutts⁷⁷, M. Cwiok³⁰, H. da Motta², A. Das⁴⁵, G. Davies⁴³, K. De⁷⁸, S.J. de Jong³⁵, E. De La Cruz-Burelo⁶⁴, C. De Oliveira Martins³, J.D. Degenhardt⁶⁴, F. Déliot¹⁸, M. Demarteau⁵⁰, R. Demina⁷¹, D. Denisov⁵⁰, S.P. Denisov³⁹, S. Desai⁵⁰, H.T. Diehl⁵⁰, M. Diesburg⁵⁰, A. Dominguez⁶⁷, H. Dong⁷², L.V. Dudko³⁸, L. Dufлот¹⁶, S.R. Dugad²⁹, D. Duggan⁴⁹, A. Duperrin¹⁵, J. Dyer⁶⁵, A. Dyshkant⁵², M. Eads⁶⁷, D. Edmunds⁶⁵, J. Ellison⁴⁸, V.D. Elvira⁵⁰, Y. Enari⁷⁷, S. Eno⁶¹, P. Ermolov³⁸, H. Evans⁵⁴, A. Evdokimov⁷³, V.N. Evdokimov³⁹, A.V. Ferapontov⁵⁹, T. Ferbel⁷¹, F. Fiedler²⁴, F. Filthaut³⁵, W. Fisher⁵⁰, H.E. Fisk⁵⁰, M. Fortner⁵², H. Fox⁴², S. Fu⁵⁰, S. Fuess⁵⁰, T. Gadfort⁷⁰, C.F. Galea³⁵, E. Gallas⁵⁰, C. Garcia⁷¹, A. Garcia-Bellido⁸², V. Gavrilov³⁷, P. Gay¹³, W. Geist¹⁹, D. Gelé¹⁹, C.E. Gerber⁵¹, Y. Gershtein⁴⁹, D. Gillberg⁶, G. Ginther⁷¹, N. Gollub⁴¹, B. Gómez⁸, A. Goussiou⁸², P.D. Grannis⁷², H. Greenlee⁵⁰, Z.D. Greenwood⁶⁰, E.M. Gregores⁴, G. Grenier²⁰, Ph. Gris¹³, J.-F. Grivaz¹⁶, A. Grohsjean²⁵, S. Grünendahl⁵⁰, M.W. Grünewald³⁰, F. Guo⁷², J. Guo⁷², G. Gutierrez⁵⁰, P. Gutierrez⁷⁵, A. Haas⁷⁰, N.J. Hadley⁶¹, P. Haefner²⁵, S. Hagopian⁴⁹, J. Haley⁶⁸, I. Hall⁶⁵, R.E. Hall⁴⁷, L. Han⁷, K. Harder⁴⁴, A. Harel⁷¹, J.M. Hauptman⁵⁷, R. Hauser⁶⁵, J. Hays⁴³, T. Hebbeker²¹, D. Hedin⁵², J.G. Hegeman³⁴, A.P. Heinson⁴⁸, U. Heintz⁶², C. Hensel^{22,d}, K. Herner⁷², G. Hesketh⁶³, M.D. Hildreth⁵⁵, R. Hirosky⁸¹, J.D. Hobbs⁷², B. Hoeneisen¹², H. Hoeth²⁶, M. Hohlfield²², S.J. Hong³¹, S. Hossain⁷⁵, P. Houben³⁴, Y. Hu⁷², Z. Hubacek¹⁰, V. Hynek⁹, I. Iashvili⁶⁹, R. Illingworth⁵⁰, A.S. Ito⁵⁰, S. Jabeen⁶², M. Jaffré¹⁶, S. Jain⁷⁵, K. Jakobs²³, C. Jarvis⁶¹, R. Jesik⁴³, K. Johns⁴⁵, C. Johnson⁷⁰, M. Johnson⁵⁰, A. Jonckheere⁵⁰, P. Jonsson⁴³, A. Juste⁵⁰, E. Kajfasz¹⁵, J.M. Kalk⁶⁰, D. Karmanov³⁸, P.A. Kasper⁵⁰, I. Katsanos⁷⁰, D. Kau⁴⁹, V. Kaushik⁷⁸, R. Kehoe⁷⁹, S. Kermiche¹⁵, N. Khalatyan⁵⁰, A. Khanov⁷⁶, A. Kharchilava⁶⁹, Y.M. Kharzhev³⁶, D. Khatidze⁷⁰, T.J. Kim³¹, M.H. Kirby⁵³, M. Kirsch²¹, B. Klima⁵⁰, J.M. Kohli²⁷, J.-P. Konrath²³, A.V. Kozelov³⁹, J. Kraus⁶⁵, D. Krop⁵⁴, T. Kuhl²⁴, A. Kumar⁶⁹, A. Kupco¹¹, T. Kurča²⁰, V.A. Kuzmin³⁸, J. Kvita⁹, F. Lacroix¹³, D. Lam⁵⁵, S. Lammers⁷⁰, G. Landsberg⁷⁷, P. Lebrun²⁰, W.M. Lee⁵⁰, A. Leflat³⁸, J. Lellouch¹⁷, J. Leveque⁴⁵, J. Li⁷⁸, L. Li⁴⁸, Q.Z. Li⁵⁰, S.M. Lietti⁵, J.G.R. Lima⁵², D. Lincoln⁵⁰, J. Linnemann⁶⁵, V.V. Lipaev³⁹, R. Lipton⁵⁰, Y. Liu⁷, Z. Liu⁶, A. Lobodenko⁴⁰, M. Lokajicek¹¹, P. Love⁴², H.J. Lubatti⁸², R. Luna³, A.L. Lyon⁵⁰, A.K.A. Maciel², D. Mackin⁸⁰, R.J. Madaras⁴⁶, P. Mättig²⁶, C. Magass²¹, A. Magerkurth⁶⁴, P.K. Mal⁸², H.B. Malbouisson³, S. Malik⁶⁷, V.L. Malyshev³⁶, H.S. Mao⁵⁰, Y. Maravin⁵⁹, B. Martin¹⁴, R. McCarthy⁷², A. Melnitchouk⁶⁶, L. Mendoza⁸, P.G. Mercadante⁵, M. Merkin³⁸, K.W. Merritt⁵⁰, A. Meyer²¹, J. Meyer^{22,d}, T. Millet²⁰, J. Mitrevski⁷⁰, R.K. Mommsen⁴⁴, N.K. Mondal²⁹, R.W. Moore⁶, T. Moulik⁵⁸, G.S. Muanza²⁰, M. Mulhearn⁷⁰, O. Mundal²², L. Mundim³, E. Nagy¹⁵, M. Naimuddin⁵⁰, M. Narain⁷⁷, N.A. Naumann³⁵, H.A. Neal⁶⁴, J.P. Negret⁸, P. Neustroev⁴⁰, H. Nilsen²³, H. Nogima³, S.F. Novaes⁵, T. Nunnemann²⁵, V. O'Dell⁵⁰, D.C. O'Neil⁶, G. Obrant⁴⁰, C. Ochando¹⁶, D. Onoprienko⁵⁹, N. Oshima⁵⁰, N. Osman⁴³, J. Osta⁵⁵, R. Otec¹⁰, G.J. Otero y Garzón⁵⁰, M. Owen⁴⁴, P. Padley⁸⁰, M. Pangilinan⁷⁷, N. Parashar⁵⁶, S.-J. Park^{22,d}, S.K. Park³¹, J. Parsons⁷⁰, R. Partridge⁷⁷, N. Parua⁵⁴, A. Patwa⁷³, G. Pawloski⁸⁰, B. Penning²³, M. Perfilov³⁸, K. Peters⁴⁴, Y. Peters²⁶, P. Pétrouff¹⁶, M. Petteni⁴³, R. Piegaia¹,

J. Piper⁶⁵, M.-A. Pleier²², P.L.M. Podesta-Lerma^{33,c}, V.M. Podstavkov⁵⁰, Y. Pogorelov⁵⁵, M.-E. Pol², P. Polozov³⁷, B.G. Pope⁶⁵, A.V. Popov³⁹, C. Potter⁶, W.L. Prado da Silva³, H.B. Prosper⁴⁹, S. Protopopescu⁷³, J. Qian⁶⁴, A. Quadt^{22,d}, B. Quinn⁶⁶, A. Rakitine⁴², M.S. Rangel², K. Ranjan²⁸, P.N. Ratoff⁴², P. Renkel⁷⁹, S. Reucroft⁶³, P. Rich⁴⁴, J. Rieger⁵⁴, M. Rijssenbeek⁷², I. Ripp-Baudot¹⁹, F. Rizatdinova⁷⁶, S. Robinson⁴³, R.F. Rodrigues³, M. Rominsky⁷⁵, C. Royon¹⁸, P. Rubinov⁵⁰, R. Ruchti⁵⁵, G. Safronov³⁷, G. Sajot¹⁴, A. Sánchez-Hernández³³, M.P. Sanders¹⁷, B. Sanghi⁵⁰, A. Santoro³, G. Savage⁵⁰, L. Sawyer⁶⁰, T. Scanlon⁴³, D. Schaile²⁵, R.D. Schamberger⁷², Y. Scheglov⁴⁰, H. Schellman⁵³, T. Schliephake²⁶, C. Schwanenberger⁴⁴, A. Schwartzman⁶⁸, R. Schwienhorst⁶⁵, J. Sekaric⁴⁹, H. Severini⁷⁵, E. Shabalina⁵¹, M. Shamim⁵⁹, V. Shary¹⁸, A.A. Shchukin³⁹, R.K. Shivpuri²⁸, V. Siccaldi¹⁹, V. Simak¹⁰, V. Sirotenko⁵⁰, P. Skubic⁷⁵, P. Slattery⁷¹, D. Smirnov⁵⁵, G.R. Snow⁶⁷, J. Snow⁷⁴, S. Snyder⁷³, S. Söldner-Rembold⁴⁴, L. Sonnenschein¹⁷, A. Sopczak⁴², M. Sosebee⁷⁸, K. Soustruznik⁹, B. Spurlock⁷⁸, J. Stark¹⁴, J. Steele⁶⁰, V. Stolin³⁷, D.A. Stoyanova³⁹, J. Strandberg⁶⁴, S. Strandberg⁴¹, M.A. Strang⁶⁹, E. Strauss⁷², M. Strauss⁷⁵, R. Ströhmer²⁵, D. Strom⁵³, L. Stutte⁵⁰, S. Sumowidagdo⁴⁹, P. Svoisky⁵⁵, A. Sznajder³, P. Tamburello⁴⁵, A. Tanasijczuk¹, W. Taylor⁶, J. Temple⁴⁵, B. Tiller²⁵, F. Tissandier¹³, M. Titov¹⁸, V.V. Tokmenin³⁶, T. Toole⁶¹, I. Torchiani²³, T. Trefzger²⁴, D. Tsybychev⁷², B. Tuchming¹⁸, C. Tully⁶⁸, P.M. Tuts⁷⁰, R. Unalan⁶⁵, L. Uvarov⁴⁰, S. Uvarov⁴⁰, S. Uzunyan⁵², B. Vachon⁶, P.J. van den Berg³⁴, R. Van Kooten⁵⁴, W.M. van Leeuwen³⁴, N. Varelas⁵¹, E.W. Varnes⁴⁵, I.A. Vasilyev³⁹, M. Vaupel²⁶, P. Verdier²⁰, L.S. Vertogradov³⁶, M. Verzocchi⁵⁰, F. Villeneuve-Segui⁴³, P. Vint⁴³, P. Vokac¹⁰, E. Von Toerne⁵⁹, M. Voutilainen^{68,e}, R. Wagner⁶⁸, H.D. Wahl⁴⁹, L. Wang⁶¹, M.H.L.S. Wang⁵⁰, J. Warchol⁵⁵, G. Watts⁸², M. Wayne⁵⁵, G. Weber²⁴, M. Weber⁵⁰, L. Welty-Rieger⁵⁴, A. Wenger^{23,f}, N. Wermes²², M. Wetstein⁶¹, A. White⁷⁸, D. Wicke²⁶, G.W. Wilson⁵⁸, S.J. Wimpenny⁴⁸, M. Wobisch⁶⁰, D.R. Wood⁶³, T.R. Wyatt⁴⁴, Y. Xie⁷⁷, S. Yacoob⁵³, R. Yamada⁵⁰, M. Yan⁶¹, T. Yasuda⁵⁰, Y.A. Yatsunenkov³⁶, K. Yip⁷³, H.D. Yoo⁷⁷, S.W. Youn⁵³, J. Yu⁷⁸, C. Zeitnitz²⁶, T. Zhao⁸², B. Zhou⁶⁴, J. Zhu⁷², M. Zielinski⁷¹, D. Zieminska⁵⁴, A. Zieminski^{54,†}, L. Zivkovic⁷⁰, V. Zutshi⁵², and E.G. Zverev³⁸

(The DØ Collaboration)

¹Universidad de Buenos Aires, Buenos Aires, Argentina

²LAFEX, Centro Brasileiro de Pesquisas Físicas, Rio de Janeiro, Brazil

³Universidade do Estado do Rio de Janeiro, Rio de Janeiro, Brazil

⁴Universidade Federal do ABC, Santo André, Brazil

⁵Instituto de Física Teórica, Universidade Estadual Paulista, São Paulo, Brazil

⁶University of Alberta, Edmonton, Alberta, Canada,

Simon Fraser University, Burnaby, British Columbia,

Canada, York University, Toronto, Ontario, Canada,

and McGill University, Montreal, Quebec, Canada

⁷University of Science and Technology of China, Hefei, People's Republic of China

⁸Universidad de los Andes, Bogotá, Colombia

⁹Center for Particle Physics, Charles University, Prague, Czech Republic

¹⁰Czech Technical University, Prague, Czech Republic

¹¹Center for Particle Physics, Institute of Physics, Academy of Sciences of the Czech Republic, Prague, Czech Republic

¹²Universidad San Francisco de Quito, Quito, Ecuador

¹³LPC, Univ Blaise Pascal, CNRS/IN2P3, Clermont, France

¹⁴LPSC, Université Joseph Fourier Grenoble 1, CNRS/IN2P3,

Institut National Polytechnique de Grenoble, France

¹⁵CPPM, Aix-Marseille Université, CNRS/IN2P3, Marseille, France

¹⁶LAL, Univ Paris-Sud, IN2P3/CNRS, Orsay, France

¹⁷LPNHE, IN2P3/CNRS, Universités Paris VI and VII, Paris, France

¹⁸DAPNIA/Service de Physique des Particules, CEA, Saclay, France

¹⁹IPHC, Université Louis Pasteur et Université de Haute Alsace, CNRS/IN2P3, Strasbourg, France

²⁰IPNL, Université Lyon 1, CNRS/IN2P3, Villeurbanne, France and Université de Lyon, Lyon, France

²¹III. Physikalisches Institut A, RWTH Aachen, Aachen, Germany

²²Physikalisches Institut, Universität Bonn, Bonn, Germany

²³Physikalisches Institut, Universität Freiburg, Freiburg, Germany

²⁴Institut für Physik, Universität Mainz, Mainz, Germany

²⁵Ludwig-Maximilians-Universität München, München, Germany

²⁶Fachbereich Physik, University of Wuppertal, Wuppertal, Germany

²⁷Panjab University, Chandigarh, India

²⁸Delhi University, Delhi, India

²⁹Tata Institute of Fundamental Research, Mumbai, India

- ³⁰ *University College Dublin, Dublin, Ireland*
- ³¹ *Korea Detector Laboratory, Korea University, Seoul, Korea*
- ³² *SungKyunKwan University, Suwon, Korea*
- ³³ *CINVESTAV, Mexico City, Mexico*
- ³⁴ *FOM-Institute NIKHEF and University of Amsterdam/NIKHEF, Amsterdam, The Netherlands*
- ³⁵ *Radboud University Nijmegen/NIKHEF, Nijmegen, The Netherlands*
- ³⁶ *Joint Institute for Nuclear Research, Dubna, Russia*
- ³⁷ *Institute for Theoretical and Experimental Physics, Moscow, Russia*
- ³⁸ *Moscow State University, Moscow, Russia*
- ³⁹ *Institute for High Energy Physics, Protvino, Russia*
- ⁴⁰ *Petersburg Nuclear Physics Institute, St. Petersburg, Russia*
- ⁴¹ *Lund University, Lund, Sweden, Royal Institute of Technology and Stockholm University, Stockholm, Sweden, and Uppsala University, Uppsala, Sweden*
- ⁴² *Lancaster University, Lancaster, United Kingdom*
- ⁴³ *Imperial College, London, United Kingdom*
- ⁴⁴ *University of Manchester, Manchester, United Kingdom*
- ⁴⁵ *University of Arizona, Tucson, Arizona 85721, USA*
- ⁴⁶ *Lawrence Berkeley National Laboratory and University of California, Berkeley, California 94720, USA*
- ⁴⁷ *California State University, Fresno, California 93740, USA*
- ⁴⁸ *University of California, Riverside, California 92521, USA*
- ⁴⁹ *Florida State University, Tallahassee, Florida 32306, USA*
- ⁵⁰ *Fermi National Accelerator Laboratory, Batavia, Illinois 60510, USA*
- ⁵¹ *University of Illinois at Chicago, Chicago, Illinois 60607, USA*
- ⁵² *Northern Illinois University, DeKalb, Illinois 60115, USA*
- ⁵³ *Northwestern University, Evanston, Illinois 60208, USA*
- ⁵⁴ *Indiana University, Bloomington, Indiana 47405, USA*
- ⁵⁵ *University of Notre Dame, Notre Dame, Indiana 46556, USA*
- ⁵⁶ *Purdue University Calumet, Hammond, Indiana 46323, USA*
- ⁵⁷ *Iowa State University, Ames, Iowa 50011, USA*
- ⁵⁸ *University of Kansas, Lawrence, Kansas 66045, USA*
- ⁵⁹ *Kansas State University, Manhattan, Kansas 66506, USA*
- ⁶⁰ *Louisiana Tech University, Ruston, Louisiana 71272, USA*
- ⁶¹ *University of Maryland, College Park, Maryland 20742, USA*
- ⁶² *Boston University, Boston, Massachusetts 02215, USA*
- ⁶³ *Northeastern University, Boston, Massachusetts 02115, USA*
- ⁶⁴ *University of Michigan, Ann Arbor, Michigan 48109, USA*
- ⁶⁵ *Michigan State University, East Lansing, Michigan 48824, USA*
- ⁶⁶ *University of Mississippi, University, Mississippi 38677, USA*
- ⁶⁷ *University of Nebraska, Lincoln, Nebraska 68588, USA*
- ⁶⁸ *Princeton University, Princeton, New Jersey 08544, USA*
- ⁶⁹ *State University of New York, Buffalo, New York 14260, USA*
- ⁷⁰ *Columbia University, New York, New York 10027, USA*
- ⁷¹ *University of Rochester, Rochester, New York 14627, USA*
- ⁷² *State University of New York, Stony Brook, New York 11794, USA*
- ⁷³ *Brookhaven National Laboratory, Upton, New York 11973, USA*
- ⁷⁴ *Langston University, Langston, Oklahoma 73050, USA*
- ⁷⁵ *University of Oklahoma, Norman, Oklahoma 73019, USA*
- ⁷⁶ *Oklahoma State University, Stillwater, Oklahoma 74078, USA*
- ⁷⁷ *Brown University, Providence, Rhode Island 02912, USA*
- ⁷⁸ *University of Texas, Arlington, Texas 76019, USA*
- ⁷⁹ *Southern Methodist University, Dallas, Texas 75275, USA*
- ⁸⁰ *Rice University, Houston, Texas 77005, USA*
- ⁸¹ *University of Virginia, Charlottesville, Virginia 22901, USA and*
- ⁸² *University of Washington, Seattle, Washington 98195, USA*

(Dated: May 22, 2008)

Data recorded by the D0 experiment at the Fermilab Tevatron Collider are analyzed to search for neutral Higgs bosons produced in association with b quarks. This production mode can be enhanced in the minimal supersymmetric standard model (MSSM). The search is performed in the three b quark channel using multijet triggered events corresponding to an integrated luminosity of 1 fb^{-1} . No statistically significant excess of events with respect to the predicted background is observed and limits are set in the MSSM parameter space.

PACS numbers: 14.80.Cp, 12.38.Qk, 12.60.Fr, 13.85.Rm

Supersymmetry (SUSY) [1] is a popular extension of the standard model (SM) which overcomes the hierarchy problem associated with electroweak symmetry breaking and the Higgs mechanism. In contrast to the SM, where only one Higgs doublet is required to break the $SU(2)$ symmetry, SUSY requires the presence of at least two Higgs doublets. In the MSSM five Higgs bosons remain after electroweak symmetry breaking; three neutral: h , H , and A - denoted as ϕ , and two charged: H^\pm . The Higgs sector can be parameterized by $\tan\beta$, the ratio of the two Higgs doublet vacuum expectation values, and m_A , the mass of the pseudo-scalar Higgs boson A .

The Higgs-quark couplings in the MSSM are proportional to their SM counterparts, with the exact factor depending on the type of quark (up- or down-type) and on the type of Higgs boson. For large values of $\tan\beta$ at least two Higgs bosons (either A and h , or A and H) have approximately the same mass and couplings to down-type quarks, which are enhanced by a factor $\tan\beta$ relative to the SM ones, while the couplings to up-type quarks are suppressed. In this large $\tan\beta$ region the three Higgs boson couplings follow the sum rule $g_{hbb}^2 + g_{Hbb}^2 + g_{Abb}^2 \approx 2 \times \tan^2\beta \times g_{hSM}^2$. In $p\bar{p}$ collisions at $\sqrt{s} = 1.96$ TeV at the Fermilab Tevatron Collider, the production of Higgs bosons associated with bottom quarks (highest mass down-type quark) is therefore, in these cases, enhanced by a factor $2 \times \tan^2\beta$ relative to the SM. Due to the $\tan\beta$ enhancement, the main decay for all these bosons is $\phi \rightarrow \bar{b}b$ (the branching fraction, $\mathcal{B}(\phi \rightarrow \bar{b}b)$, is $\approx 90\%$). The enhanced production and branching ratio make the final state with three b jets an important channel in the search for MSSM Higgs bosons at large $\tan\beta$. At a hadron collider this final state has a large background from multijet production which is poorly modeled by simulation, making the search for this topology very challenging.

MSSM Higgs boson production has been studied at LEP which excluded $m_{h,A} < 93$ GeV/ c^2 for all $\tan\beta$ values [2]. CDF [3, 4] and D0 [5, 6] have extended the MSSM Higgs boson searches to higher masses for high $\tan\beta$ values. The result presented in this Letter supersedes our previous published result [5]. In addition to including more data, this analysis benefits from improved signal and background modeling and an improved limit setting procedure, which uses only the shape, and not the normalization, of the final discriminating variable.

The D0 detector is described in Ref. [7]. Dedicated triggers designed to select events with at least three jets are used in this analysis. Typical requirements are at least two jets with transverse momenta $p_T > 25$ GeV/ c , an additional jet with $p_T > 15$ GeV/ c , and the $p\bar{p}$ interaction vertex is required to be reconstructed well within the geometric acceptance of the silicon detector. Algorithms for identifying b jets at the trigger level are also employed in about 70% of the integrated luminosity used for this analysis. After data quality requirements the total data

sample corresponds to 1.02 ± 0.06 fb $^{-1}$ [8].

Signal samples are generated for Higgs boson masses from 90-220 GeV/ c^2 using the leading order PYTHIA event generator [9] to generate associated production of ϕ and a b quark in the 5-flavor scheme, $gb \rightarrow \phi b$. Weights, calculated with MCFM [10], are applied to the signal samples as a function of p_T and η of the leading b jet which is not from the decay of the Higgs boson, to correct the cross section and experimental acceptance to next-to-leading order (NLO). Multijet background events from the $b\bar{b}$, $b\bar{b}j$, $b\bar{b}jj$, $c\bar{c}$, $c\bar{c}j$, $c\bar{c}jj$, $b\bar{b}c\bar{c}$, and $b\bar{b}b\bar{b}$ processes (where j denotes a light parton: u , d , s quark or gluon) are generated with the ALPGEN [11] event generator. The contributions from other processes, such as $t\bar{t}$, $Zb\bar{b}$, and single top production, are found to be negligible. The ALPGEN samples are processed through PYTHIA for showering and hadronization. All samples are then processed through a GEANT-based [12] simulation of the D0 detector and the same reconstruction algorithms as the data. A parameterized trigger simulation is used to model the effects of the trigger requirements on the simulated events.

Jets are reconstructed from energy deposits in calorimeter towers using the midpoint cone algorithm [13] with radius = 0.5. Jet reconstruction and energy scale determination are described in detail in Ref. [14]. All calorimeter jets are required to pass a set of quality criteria with about 98% efficiency and have at least two reconstructed tracks within $\Delta\mathcal{R}(\text{track}, \text{jet-axis}) = \sqrt{(\Delta\eta)^2 + (\Delta\varphi)^2} < 0.5$ (where η is the pseudorapidity and φ the azimuthal angle).

We select signal events by requiring at least three and at most five jets with $p_T > 20$ GeV/ c and $|\eta| < 2.5$. A neural network (NN) based b -tagging algorithm [15], with lifetime based information involving the track impact parameters and secondary vertices as inputs, is used to identify b jets. Each event must have at least three jets satisfying a tight b -tag NN requirement. The single jet b -tagging efficiency is $\approx 50\%$ for a light-jet mistag rate of $\approx 0.4\%$. The events with at least two tight b -tags are also kept and used to model the background. Simulated events are weighted based on their tagging and fake rate probabilities determined from data. Finally, the transverse momenta of the two highest p_T jets which are also b -tagged are required to be above 25 GeV/ c . To further increase the sensitivity, the analysis is split into separate three-, four-, and five-jet channels. After the event selection 3,224 events remain in the exclusive three-jet sample, 2,503 and 704 events, respectively, in the four- and five-jet sample. The signal efficiencies for Higgs boson masses between 100 and 200 GeV/ c^2 range from 0.3 – 1.2% in the three-jet channel (0.2 – 0.6% and 0.01 – 0.12% in the four- and five-jet channels).

The background composition is determined separately for each jet multiplicity. The fractional contribution α_i of the i th background process is calculated from equations linking the b -tag efficiency, ϵ_j , in an event with the N_j

observed events:

$$\begin{aligned} \sum_i \alpha_i &= 1 \\ \sum_i \alpha_i \times \epsilon_j^i &= N_j/N_{\text{tot}} \end{aligned} \quad (1)$$

Here, j indicates single, double and triple b -tagged jets in an event for different b -tag criteria, and N_{tot} is the total number of events. The double b -tagged sample is found to be dominated by $b\bar{b}j$ while the triple b -tagged sample consists of a mix of $\approx 50\%$ $b\bar{b}b$, $\approx 30\%$ $b\bar{b}j$, and $\approx 20\%$ $b\bar{b}c + b\bar{c}b$. An alternative method to determine the background, based on fitting simulated $H_T = \sum p_{T_{\text{jet}}}$ shape templates to the data, confirms the composition of the background.

For every event the two jet pairs with the largest summed transverse momenta are considered as possible Higgs boson candidates. To remove discrepancies between data and simulation originating from gluon splitting ($g \rightarrow b\bar{b}$), only jet pairs with $\Delta\mathcal{R} > 1.0$ are considered in the final analysis.

The following six variables separate the signal from the backgrounds and are well modeled by the simulation: the difference in pseudorapidity between the two jets in the pair; the azimuthal angular difference between the two jets in the pair; the angle between the leading jet in the pair and the total momentum of the pair; $|p_{\vec{v}_1} - p_{\vec{v}_2}|/|p_{\vec{v}_1} + p_{\vec{v}_2}|$, the momentum balance in the pair; the rapidity of the pair; and the event sphericity. Based on these kinematic variables, a likelihood discriminant \mathcal{D} , is calculated according to:

$$\mathcal{D}(x_1, \dots, x_6) = \frac{\prod_{i=1}^6 p_i^{\text{sig}}(x_i)}{\prod_{i=1}^6 p_i^{\text{sig}}(x_i) + \prod_{i=1}^6 p_i^{\text{bkg}}(x_i)}, \quad (2)$$

where p_i^{sig} (p_i^{bkg}) refers to the signal (background) probability density function (pdf) for variable x_i , and (x_1, \dots, x_6) is the set of measured kinematic variables for the jet pair. The pdfs are obtained from triple b -tagged signal and background simulation. Two likelihoods are built combining simulated samples in the 90–130 GeV/ c^2 (“Low-mass”) and 130–220 GeV/ c^2 (“High-mass”) mass ranges, providing discrimination at low and high masses, respectively. Studies show that this division of the mass range gives the best discrimination.

Several multijet processes contribute to the background and the uncertainty on the cross sections is large. The $b\bar{b}b$ component may also contain a contribution that is indistinguishable from a signal and cannot be normalized from the data. To model the background we therefore rely on a combination of data and simulation. The distribution of the expected triple b -tagged (3Tag) sample in the two-dimensional \mathcal{D} and invariant mass (M_{bb}) plane, $S_{3\text{Tag}}^{\text{exp}}(\mathcal{D}, M_{bb})$, is obtained from the double b -tagged (2Tag) data shape multiplied by the ratio of the simulated (MC) shapes of the triple and double tagged

events:

$$S_{3\text{Tag}}^{\text{exp}}(\mathcal{D}, M_{bb}) = \frac{S_{3\text{Tag}}^{\text{MC}}(\mathcal{D}, M_{bb})}{S_{2\text{Tag}}^{\text{MC}}(\mathcal{D}, M_{bb})} S_{2\text{Tag}}^{\text{data}}(\mathcal{D}, M_{bb}). \quad (3)$$

Many uncertainties affecting the simulation cancel in the ratio $\frac{S_{3\text{Tag}}^{\text{MC}}(\mathcal{D}, M_{bb})}{S_{2\text{Tag}}^{\text{MC}}(\mathcal{D}, M_{bb})}$. Figure 1 shows \mathcal{D} for data and background for the low-mass likelihood in the three-jet channel.

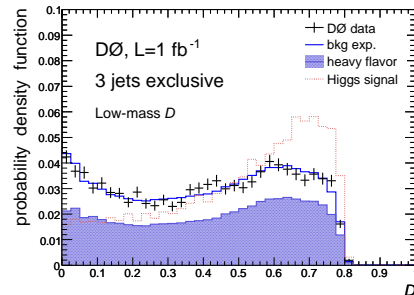


FIG. 1: Comparison of the low-mass likelihood distributions for the 3Tag data and background (bkg exp.) defined by Eq. 3. Every event has two entries. Black crosses refer to data, the solid line shows the total background estimate, and the shaded region represents the heavy flavor component ($b\bar{b}b$, $b\bar{b}c$, and $c\bar{c}b$). The distribution for a Higgs boson of mass 100 GeV/ c^2 is also shown.

The selection cuts on \mathcal{D} , b -tagging, and number of jet-pair combinations per event are optimized by maximizing the expected sensitivity. The optimal cuts for the likelihood vary between 0.25 and 0.60 depending on the jet multiplicity and Higgs boson mass. The agreement of the data and the background expectation is verified in a control region where the impact of any Higgs boson signal is limited, defined by $\mathcal{D} < 0.25$. The agreement is also verified in the case when no likelihood cut is applied. Figure 2 shows the invariant mass for the optimized high-mass likelihood cuts.

Several sources of systematic uncertainties affecting the background shape through the ratio $\frac{S_{3\text{Tag}}^{\text{MC}}(\mathcal{D}, M_{bb})}{S_{2\text{Tag}}^{\text{MC}}(\mathcal{D}, M_{bb})}$ in Eq. 3 are considered. The dominant uncertainty, due to the background composition, is estimated by varying the ratio of $b\bar{b}j$ and $b\bar{b}b$ events in the sample corresponding to the uncertainties from the background composition fit. In addition, the smaller uncertainties from the kinematic dependence of the b -tagging, the b jet energy resolution, the $b\bar{b}b$ and $b\bar{b}j$ kinematics, and finally the trigger-level b -tag requirement were also evaluated and included in the systematic uncertainty on the background shape.

The Modified Frequentist method [16] is used to estimate the compatibility of the data with the background-only hypothesis ($1 - CL_b$) as well as to derive limits at the 95% C.L. on the cross section times branching ratio

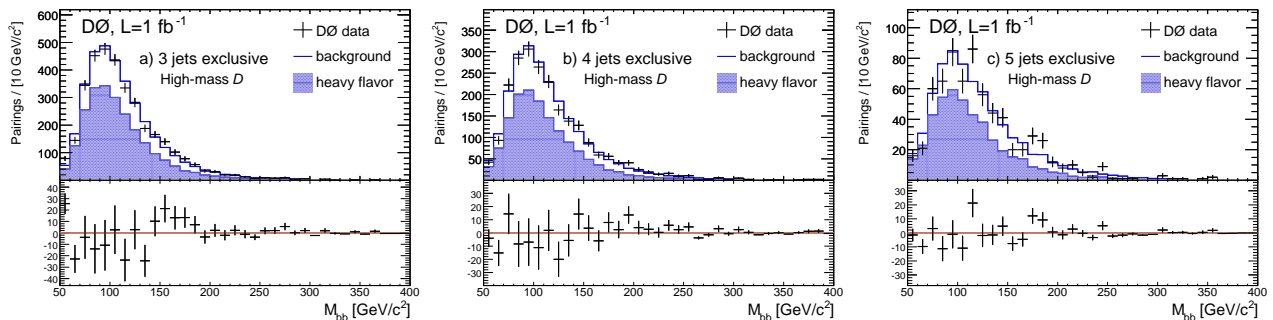


FIG. 2: Invariant mass for the high-mass likelihood region for the exclusive a) three-jet b) four-jet, and c) five-jet channels. Black crosses refer to data, the solid line shows the total background estimate, and the shaded region represents the heavy flavor component ($b\bar{b}$, $b\bar{c}$, and $c\bar{c}$). The lower panels show the difference between the data and the background expectation.

as a function of m_A . Only the shapes (not the normalization) of the M_{bb} distributions are used to discriminate signal from background, assuming the width of ϕ to be narrow relative to the experimental resolution. Table I shows the limits and the $1 - CL_b$ values obtained versus the hypothesized Higgs boson mass. The low $1 - CL_b$

Mass (GeV/ c^2)	$\sigma \times \mathcal{B}$ Exp.(pb)	$\sigma \times \mathcal{B}$ Obs.(pb)	$1 - CL_b$ (in %)
90	170^{+72}_{-52}	184	39
100	117^{+48}_{-35}	128	38
110	71^{+35}_{-20}	69	52
120	41^{+18}_{-9}	34	73
130	28^{+12}_{-7}	24	70
140	25^{+11}_{-6}	22	60
160	17^{+8}_{-4}	26	12
180	13^{+5}_{-3}	23	4.4
200	9^{+4}_{-3}	17	7.0
220	7^{+3}_{-2}	12	12

TABLE I: Cross section limits as a function of Higgs boson mass. Columns two and three show the expected (Exp.) and observed (Obs.) limits on the cross section times branching fraction to $b\bar{b}$. The total one-sigma uncertainty on the expected limits is also displayed. The last column shows the value of $1 - CL_b$.

values around a Higgs mass of 180 GeV/ c^2 are due to a slight excess over the expected SM background.

The results of this search can be used to set limits on the parameters of the MSSM. As a consequence of the enhanced couplings to b quarks at large $\tan\beta$ the total width of the neutral Higgs bosons also increases with $\tan\beta$. This can have an impact on our search if the width is comparable to or larger than the experimental resolution of the reconstructed invariant mass of a di-jet system. To take this effect into account, the width of the Higgs boson is calculated with FEYNHIGGS [17] and included in the simulation as a function of the mass and $\tan\beta$ by convoluting a relativistic Breit-Wigner function

with the NLO cross section. In the MSSM the masses and couplings of the Higgs bosons depend, in addition to $\tan\beta$ and m_A , on the SUSY parameters through radiative corrections. Limits on $\tan\beta$ as a function of m_A are derived for two particular scenarios assuming a CP-conserving Higgs sector [18]: the m_h^{\max} scenario and the no-mixing scenario. Since the results depend considerably upon the Higgs sector bilinear coupling μ , its two possible signs are also probed.

Figure 3 shows the results obtained in the present analysis interpreted in these different MSSM scenarios. Substantial areas in the MSSM parameter phase space up to masses of 200 GeV/ c^2 are excluded. No exclusion can be obtained for the m_h^{\max} , $\mu > 0$ scenario. This analysis extends the mass range over which the search is performed. In addition these results benefit from NN b -tagging and a likelihood discriminant as well as improved modeling and a robust limit setting procedure, using only the shape of the discriminating variable.

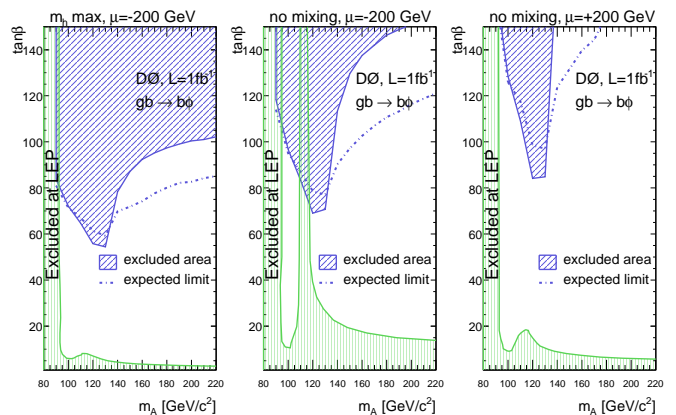


FIG. 3: 95% C.L. exclusion limits in the $(m_A, \tan\beta)$ plane for m_h^{\max} , $\mu = -200$ GeV, and no-mixing, $\mu = -200$ GeV and $\mu = +200$ GeV. The exclusions from LEP are also shown [2]. The width of ϕ is larger than 70% of m_A above $\tan\beta = 100$ in the m_h^{\max} , $\mu = -200$ GeV scenario.

We thank the staffs at Fermilab and collaborating institutions, and acknowledge support from the DOE and NSF (USA); CEA and CNRS/IN2P3 (France); FASI, Rosatom and RFBR (Russia); CNPq, FAPERJ, FAPESP and FUNDUNESP (Brazil); DAE and DST (India); Colciencias (Colombia); CONACyT (Mexico); KRF and KOSEF (Korea); CONICET and UBACyT (Argentina); FOM (The Netherlands); STFC (United Kingdom); MSMT and GACR (Czech Republic); CRC Program, CFI, NSERC and WestGrid Project (Canada); BMBF and DFG (Germany); SFI (Ireland); The Swedish Research Council (Sweden); CAS and CNSF (China); and the Alexander von Humboldt Foundation.

-
- [a] Visitor from Augustana College, Sioux Falls, SD, USA.
 [b] Visitor from The University of Liverpool, Liverpool, UK.
 [c] Visitor from ICN-UNAM, Mexico City, Mexico.
 [d] Visitor from II. Physikalisches Institut, Georg-August-University, Göttingen, Germany.
 [e] Visitor from Helsinki Institute of Physics, Helsinki, Finland.
 [f] Visitor from Universität Zürich, Zürich, Switzerland.
 [‡] Deceased.

- [1] H.P. Nilles, Phys. Rep. **110**, 1 (1984); H.E. Haber and G.L. Kane, Phys. Rep. **117**, 75 (1985).
 [2] S. Schael *et al.* (The ALEPH, DELPHI, L3, and OPAL Collaborations), Eur. Phys. J. C **47**, 547 (2006).

- [3] T. Affolder *et al.* (CDF collaboration), Phys. Rev. Lett. **86**, 4472 (2001).
 [4] A. Abulencia *et al.* (CDF Collaboration), Phys. Rev. Lett. **96**, 011802 (2006).
 [5] V.M. Abazov *et al.* (D0 Collaboration), Phys. Rev. Lett. **95**, 151801 (2005).
 [6] V.M. Abazov *et al.* (D0 Collaboration), arXiv:hep-ex/0805.2491 (2008).
 [7] V.M. Abazov *et al.* (D0 Collaboration), Nucl. Instrum. Methods Phys. Res. A **565**, 463 (2006).
 [8] T. Andeen *et al.*, FERMILAB-TM-2365 (2007).
 [9] T. Sjöstrand *et al.*, arXiv:hep-ph/0308153 (2003).
 [10] J. Campbell, R.K. Ellis, F. Maltoni, and S. Willenbrock, Phys. Rev. D **67**, 095002 (2003).
 [11] M.L. Mangano *et al.*, J. High Energy Phys. **307**, 001 (2003).
 [12] R. Brun and F. Carminati, CERN program library long writeup W5013 (1993).
 [13] G. Blazey *et al.*, arXiv:hep-ex/0005012 (2000).
 [14] V.M. Abazov *et al.* (D0 Collaboration), Fermilab-Pub-08/034-E (2008).
 [15] T. Scanlon, FERMILAB-THESIS-2006-43.
 [16] T. Junk, Nucl. Instrum. Methods Phys. Res. A **434**, 435 (1999); A. Read, Nucl. Instrum. Methods Phys. Res. A **425**, 357 (1999).
 [17] S. Heinemeyer, W. Hollik, and G. Weiglein, Eur. Phys. J. C **9**, 343 (1999); Comput. Phys. Commun. **124**, 76 (2000); G. Degrandi *et al.*, Eur. Phys. J. C **28**, 133 (2003), M. Frank *et al.*, JHEP **0702**, 047 (2007). We used FEYNHIGGS version 2.6.3.
 [18] M. Carena, S. Heinemeyer, C. E. M. Wagner, and G. Weiglein, Eur. Phys. J. C **45**, 797 (2006).